SIMS analyses of the oldest known assemblage of microfossils document their taxon-correlated carbon isotope compositions

J. William Schopf[a,b,c,d,1], Kouki Kitajima[d], Michael J. Spicuzza[d], Anatoliy B. Kudryavtsev[b], and John W. Valley[d]

[a]Department of Earth, Planetary, and Space Sciences, University of California, Los Angeles, CA 90095; [b]Center for the Study of Evolution and the Origin of Life, University of California, Los Angeles, CA 90095; [c]Molecular Biology Institute, University of California, Los Angeles, CA 90095; and [d]Wisconsin Astrobiology Research Consortium, Department of Geoscience, University of Wisconsin, Madison, WI 53706

Contributed by J. William Schopf, November 17, 2017 (sent for review October 16, 2017; reviewed by David J. Bottjer, Andrew Czaja, and Yanan Shen)

Analyses by secondary ion mass spectroscopy (SIMS) of 11 specimens of five taxa of prokaryotic filamentous kerogenous cellular microfossils permineralized in a petrographic thin section of the ∼3,465 Ma Apex chert of northwestern Western Australia, prepared from the same rock sample from which this earliest known assemblage of cellular fossils was described more than two decades ago, show their $\delta^{13}C$ compositions to vary systematically taxon to taxon from −31‰ to −39‰. These morphospecies-correlated carbon isotope compositions confirm the biogenicity of the Apex fossils and validate their morphology-based taxonomic assignments. Perhaps most significantly, the $\delta^{13}C$ values of each of the five taxa are lower than those of bulk samples of Apex kerogen (−27‰), those of SIMS-measured fossil-associated dispersed particulate kerogen (−27.6‰), and those typical of modern prokaryotic phototrophs (−25 ± 10‰). The SIMS data for the two highest $\delta^{13}C$ Apex taxa are consistent with those of extant phototrophic bacteria; those for a somewhat lower $\delta^{13}C$ taxon, with nonbacterial methane-producing Archaea; and those for the two lowest $\delta^{13}C$ taxa, with methane-metabolizing γ-proteobacteria. Although the existence of both methanogens and methanotrophs has been inferred from bulk analyses of the carbon isotopic compositions of pre-2,500 Ma kerogens, these in situ SIMS analyses of individual microfossils present data interpretable as evidencing the cellular preservation of such microorganisms and are consistent with the near-basal position of the Archaea in rRNA phylogenies.

Apex chert | Archaea | Archean | methanogens | methanotrophs

Widely regarded as among the oldest known evidence of life, the morphologically diverse cellular carbonaceous (kerogenous) microscopic fossils of the ∼3,465 Ma Apex chert, systematically described more than two decades ago (1, 2), have been a focus of controversy. Perhaps spurred by a reluctance to affirm the veracity of "claims for life in the earliest 2.0–2.5 billion years of Earth's history" (3), some workers have suggested the Apex fossils to be chert-embedded mineralic pseudofossils composed of "abiotic graphite" (4, 5), barium carbonate (6, 7), or hematite in secondary veinlets (8). Other studies implied that the fossils are nonindigenous clay mineral needle-like crystallites (9) or suggested them to be composed of "vermiculate-like" minerals produced via a "nonbiological formation model" involving the hydration and exfoliation of mica flakes followed by their surficial adsorption of later-introduced hydrocarbons (10).

Principal deficiencies of these suggestions are that carbonaceous (kerogenous) cellular microbe-like assemblages of nonbiologic pseudofossils are evidently unknown in the geological record; abiologically produced kerogenous particulate organic matter is similarly unreported from the geological record; and virtually none of these studies is reported to have been based on examination of the scores of demonstrably kerogenous (4, 11, 12) morphometrically diverse well-characterized (1, 2) originally described Apex specimens archived at London's Natural History Museum (NHM) (2).

Although the earlier disputed biogenicity of the Apex fossils seems largely to have been laid to rest (12), the biological affinities and physiological characteristics of these exceedingly ancient fossil microbes remain to be established. Initially formally described as "prokaryotes *Incertae Sedis*"—nonnucleated microorganisms of uncertain and undefined systematic relations (ref. 2, p. 643)—the present study suggests a solution to this unresolved problem.

We here present results of in situ analyses of 11 specimens of five taxa of permineralized microscopic fossils embedded in Apex chert petrographic thin section 4 of 6/15/82-1H prepared from the same rock sample at the same time as the six holotype- and paratype-containing sections previously archived at the NHM (sections 4 of 6/15/82-1B through 6/15/82-1G; refs. 1 and 2). The indigenousness and syngenicity of the permineralized fossils to their encompassing chert matrix is shown by optical microscopy supported by Raman spectroscopy which also establishes their kerogenous composition. The biogenicity and taxonomic relations of the analyzed fossils are documented by their demonstrably cellular cylindrical filamentous morphology; the taxon-defining size ranges of their medial cells and, where preserved, the morphology of their terminal cells; and their morphometric comparison with previously reported specimens from the same rock. Analyses of each of the 11 specimens by secondary ion mass spectroscopy (SIMS) document the carbon isotope compositions of the five taxa studied.

The taxon-correlated SIMS carbon isotope data reported here reaffirm the carbonaceous, kerogenous (rather than mineralic)

Significance

Although the existence of the Archaea (one of three all-encompassing domains of life) in the Archean Eon (4,000 to 2,500 million years ago) has been inferred from carbon isotopes in bulk samples of ancient rocks, their cellular fossils have been unknown. We here present carbon isotope analyses of 11 microbial fossils from the ∼3,465-million-year-old Western Australian Apex chert from which we infer that two of the five species studied were primitive photosynthesizers, one was an Archaeal methane producer, and two others were methane consumers. This discovery of Archaea in the Archean is consistent with the rRNA "tree of life," confirms the earlier disputed biogenicity of the Apex fossils, and suggests that methane-cycling methanogen–methanotroph communities were a significant component of Earth's early biosphere.

Author contributions: J.W.S., K.K., M.J.S., and J.W.V. designed research; J.W.S., K.K., M.J.S., A.B.K., and J.W.V. performed research; J.W.S., K.K., M.J.S., and J.W.V. analyzed data; and J.W.S. and J.W.V. wrote the paper.

Reviewers: D.J.B., University of Southern California; A.C., University of Cincinnati; and Y.S., University of Science and Technology of China.

The authors declare no conflict of interest.

[1]To whom correspondence should be addressed. Email: schopf@epss.ucla.edu.

This article contains supporting information online at www.pnas.org/lookup/suppl/doi:10.1073/pnas.1718063115/-/DCSupplemental.

composition of the exceedingly ancient Apex fossils; reinforce the widely assumed (but difficult to firmly establish) validity of the use of cellular and organismal morphology for the assignment of ancient microbes to biologically meaningful taxonomic categories; and provide insight into the physiology and biological affinities of the five Apex taxa examined.

Results and Discussion

Geologic Setting. Geologically initially mapped as a shallow marine facies (13, 14), the fossiliferous locality (3) of the ∼3,465 Ma Apex chert (15) has more recently been reinterpreted to be a brecciated and altered hydrothermal vein deposit (16). The 11 specimens of five taxa of permineralized microscopic fossils analyzed here are embedded in Apex chert petrographic thin section 4 of 6/15/82-1H prepared from a rock sample collected from outcrop in 1982 (cf. refs. 1 and 2).

Although a hydrothermal environment has been suggested to be unlikely for preservation of delicate fossil microbes (4, 5, 9), biota-prohibiting hydrothermal temperatures for the genesis of the Apex chert have not been demonstrated; microorganisms morphologically comparable to the Apex filaments are common in modern hydrothermal settings (17); filamentous microbes similar to *Primaevifilum amoenum*, the most abundant of the described Apex taxa (2), have long been known to occur at deep-sea thermal vents (18); and chert-permineralized fossil filaments, including specimens so similar to those of the Apex chert that they have been assigned to two of the Apex taxa (19) are present in three other Paleoarchean hydrothermal units of the northwestern Australian Pilbara Craton (19–24).

Specimens Analyzed. The locations of the 11 SIMS-analyzed Apex microfossils in chert thin section 4 of 6/15/82-1H are shown in Fig. 1 *A–N* compared with three previously described Apex specimens (Fig. 1 *P–Z*) permineralized in NHM-archived thin section 4 of 6/15/82-1B (2).

As is shown (Fig. 1 *A*, *E*, *H*, and *O*), the Apex fossils typically occur in subrounded millimeter-sized carbonaceous chert clasts in which they are embedded in flocculent organic matter. Within such clasts, the Apex fossils are commonly rather closely spaced, numerous specimens occurring within a given granular clast (Fig. 1 *H–N* and *P–S*). Optical photomicrographs (e.g., Fig. 1 *D* and *Q–S*) and 3D (Fig. 1*T*) and 2D (Fig. 1 *U–Z*) Raman images of the fossils show them to be cellular, exhibiting box-like cell lumina-enclosing kerogenous cell walls.

Like some of the microfossils permineralized in other Paleoarchean hydrothermal units, it is possible that the Apex filaments represent remnants of thermophilic microbes preserved in situ. Given their clast-embedded mode of occurrence, however, it seems more likely that the fossils are allocthonous to the deposit, older than or penecontemporaneous with the Apex chert, fossilized microbes emplaced in the unit in reworked detrital carbonaceous granules.

Data documenting the carbonaceous (kerogenous) composition of each of the 11 SIMS-analyzed Apex specimens are shown in Fig. 2, 2D Raman images acquired at the kerogen "G" band (∼1,605 cm^{-1}) accompanied by optical photomicrographs of the specimens studied. Such data, acquired routinely to differentiate bona fide microfossils from mineralic "fossil-like" microscopic objects, provided the biogenic targets for subsequent SIMS analyses.

Fig. 3 and Dataset S1 present pre- and post-SIMS images of the Apex fossils discussed here, showing that the SIMS-analyzed pits spatially correspond to the specimens exposed at the surface of the polished thin section. Table 1 summarizes the SIMS-measured $\delta^{13}C$ values of the 11 specimens of the five taxa analyzed. Details regarding SIMS analyses of these specimens, measurements that we regard as among the most reliable reported for microfossils in chert, are documented in *Supporting Information*.

Biological Affinities of the Apex Fossils. SIMS $\delta^{13}C$ data for the 11 Apex fossils analyzed (Figs. 1–3 and Table 1) provide a means to assess the physiology and biological affinities of the five taxa studied. The $\delta^{13}C$ values of the individual fossils reported here range from −29.8‰ to −44.1‰ (Table 1), the data showing that each of the five morphometrically defined taxa has a characteristic carbon isotope composition that varies taxon to taxon from the highest in $\delta^{13}C$ (an unnamed unicell, −30.9‰, and *Primaevifilum minutum*, −31.6‰) to the lowest (*Archaeocillatoriopsis disciformis*, −39.2‰, and *P. amoenum*, −39.4‰). The SIMS-determined $\delta^{13}C$ values of the fossils thus differ from those of bulk samples of Apex kerogen (−27‰; ref. 25) and those of SIMS measurements acquired away from the fossils to determine the $\delta^{13}C$ values of particulate kerogen dispersed in the chert matrix (∼−27.6‰; Table S1 and Dataset S2).

As discussed below, the microfossil $\delta^{13}C$ values are similar to those of extant prokaryotic phototrophs, methanogenic Archaeans, and γ-proteobacterial methanotrophs.

Direct evidence of the biological affinities of the Apex fossils is limited to their (*i*) cellular and organismal morphologies and (*ii*) SIMS-measured carbon isotope ratios, the plausibility of the resulting interpretations being evaluated by (*iii*) the similarity of their morphologies and $\delta^{13}C$ values to extant microorganisms and their consonance with inferences based on (*iv*) available geochemical and fossil data from comparably ancient sediments and (*v*) the position of the inferred biological lineages on the phylogenic rRNA "tree of life." As noted above, for these evidently allocthonous clast-embedded specimens (Fig. 1), a sixth typically relevant criterion, their original ecological setting, cannot currently be accurately assessed.

Below, we evaluate the biological affinities of the Apex taxa in three categories ordered by their SIMS-determined highest to lowest average $\delta^{13}C$ values (Table 1).

i) Specimens exhibiting the highest $\delta^{13}C$ values measured include an unnamed unicell ($\delta^{13}C$ −30.9‰; Figs. 1*N*, 2 *U* and *V*, and 3 *I* and *J*) and three specimens of *P. minutum* ($\delta^{13}C$ −31.6‰; Figs. 1 *F, G,* and *K*, 2 *O–T*, and 3 *E, F,* and *S–V*). Extant prokaryotic phototrophs have $\delta^{13}C$ values reported to range, for cyanobacteria, from −8‰ to −31‰, and, for non-oxygenic photosynthetic bacteria, from −19‰ to −36‰ (26). The ranges of $\delta^{13}C$ values of the three analyzed specimens of the unnamed unicell and *P. minutum* overlap with the $\delta^{13}C$ values of such extant phototrophs, their morphologies also being similar to those of diverse modern (27) and Precambrian mat-building (stromatolitic) microbial phototrophs, both Archean (e.g., refs. 24 and 28) and Paleoproterozoic (e.g., ref. 29), in which, as we infer for the organic-rich clasts of the Apex chert, microbes of diverse physiologies cooccur on a millimetric scale.

ii) One taxon, *P. delicatulum*, represented by four analyzed specimens, has a lower average $\delta^{13}C$ value of −35.4‰ (Figs. 1 *I–M*, 2 *K–N*, and 3 *E–H* and *K–N*). Although the average $\delta^{13}C$ value of the four specimens of this taxon analyzed marginally overlaps with the lowest values recorded for extant anoxygenic phototrophs (−36‰; ref. 26), their range of carbon isotope values (32.7 to −38.2‰; Table 1) is particularly similar to that of modern methanogenic Archaeans (−27‰ to −38‰; ref. 26). Nevertheless, the cellular 1.8- to 3.2-μm-broad filaments of *P. delicatulum* (2) differ markedly in morphology from described methanogens, almost all such modern taxa being composed of spherical, rod-shaped, or rectangular single cells. The sole filamentous methanogen yet reported, *Thermofilum*, is characterized by thin straight or curved filaments 0.1 to 0.3 μm broad (30, 31) and, thus, is unlike the much broader filaments of the Apex taxon. This apparent absence of a modern morphological analog of *P. delicatulum* may reflect the relatively recent, 1990 recognition of the Archaea Domain (32) and a resulting lack of comprehensive surveys of extant members of the group or, perhaps, the possibility that the ∼3,465 Ma Apex taxon represents an early-evolved but now extinct Archaeal lineage.

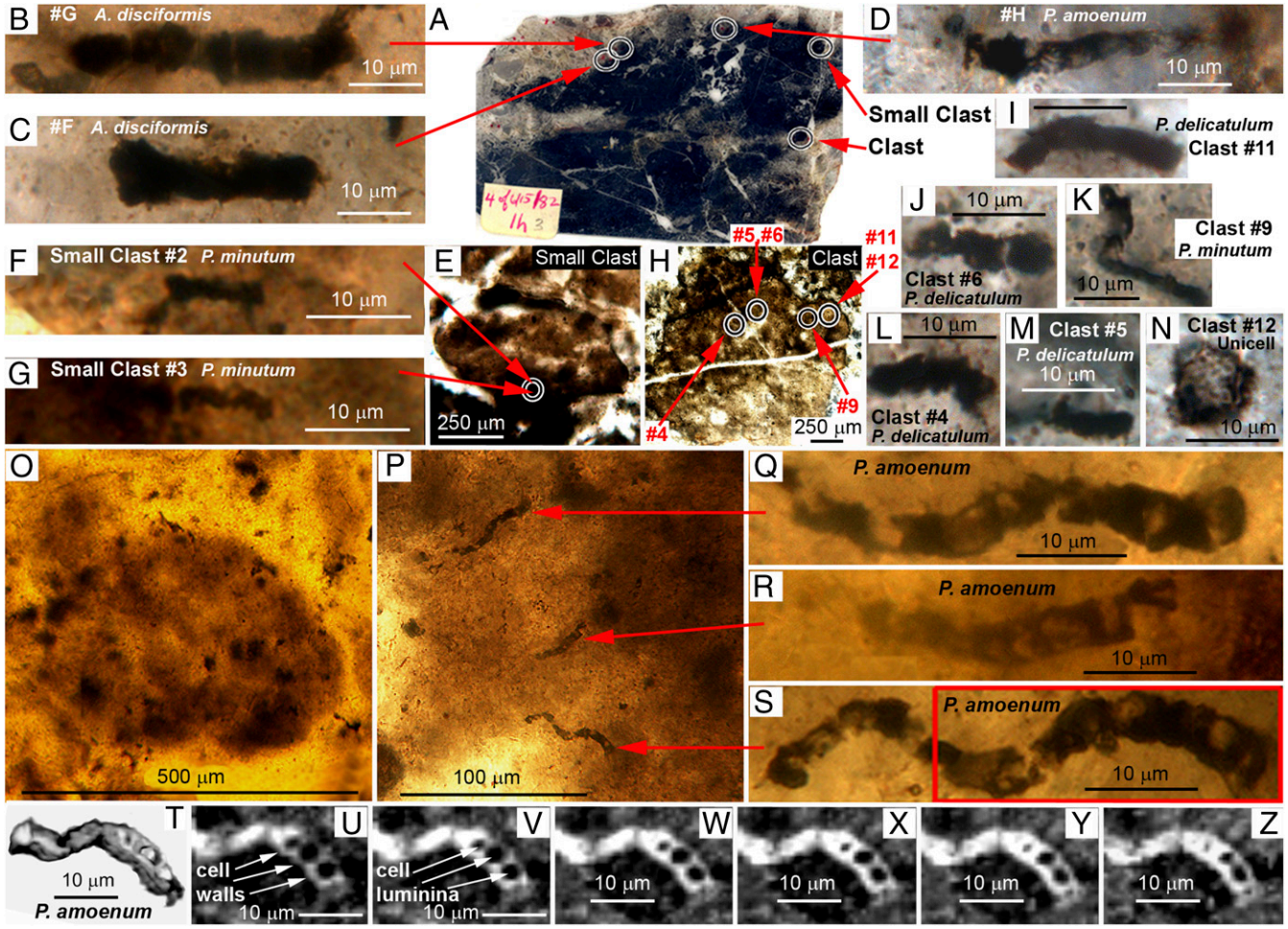

Fig. 1. (*A–N*) Optical photomicrographs showing the locations of (*B–D*, *F*, *G*, *I–N*) 11 specimens of five taxa of microfossils analyzed by SIMS embedded in clouds of flocculent organic matter permineralized in (*A*) petrographic thin section 4 of 6/15/82-1H of the ∼3,465 Ma Apex chert and (*E* and *H*) in its contained subrounded carbonaceous clasts. (*O–S*) Optical photomicrographs of (*O*) a similar clast and (*P–S*) filamentous microfossils in petrographic thin section 4 of 6/15/82-1B archived at London's NMH (2). (*T*) 3D and (*U–Z*) 2D Raman images of the part of the specimen enclosed by the red rectangle in *S*. (*A*) Thin section 4 of 6/15/82–1H. (*B* and *C*) *A. disciformis* Schopf 1993 (specimens #G and #F, respectively). (*D*) *P. amoenum* Schopf 1992 (specimen #H). (*E*) Small clast. (*F*, *G*, and *K*) *P. minutum* Schopf 1993 (small clast specimens #2 and #3, and clast specimen #9, respectively). (*H*) Clast. (*I*, *J*, *L*, and *M*) *P. delicatulum* Schopf 1992 (clast specimens #11, #6, #4, and #5, respectively). (*N*) Unnamed unicell (clast specimen #12). (*O*) A subrounded carbonaceous clast. (*P–S*) Organic clast-enclosed specimens of *P. amoenum*, the arrows in *P* denoting their locations within the clast. (*T–Z*) Raman images (acquired in a spectral window centered on the kerogen "G" band at ∼1,605 cm^{-1}) in which the 3D image in *T* has been rotated to show the cylindrical morphology of the filament and *U–Z* show 2D images at increasing depths through the specimen (*U*, 0.75 μm; *V*, 1.5 μm; *W*, 2.25 μm; *X*, 3.0 μm; *Y*, 3.75 μm; *Z*, 4.0 μm) that document its box-like kerogenous cell walls (arrows in *U*) and their enclosed cell lumina (arrows in *V*).

iii) The lowest $\delta^{13}C$ values measured are exhibited by two specimens of *A. disciformis* ($\delta^{13}C$ −39.2‰; Figs. 1 *B* and *C*, 2 *A–D*, and 3 *K–P*) and one specimen of *P. amoenum* ($\delta^{13}C$ −39.4‰; Figs. 1*D*, 2 *I* and *J*, and 3 *Q* and *R*). Relative to extant prokaryotic phototrophs and methanogens, the SIMS-measured carbon isotope values of the three specimens comprising this grouping are appreciably lower. Characteristically low $\delta^{13}C$ Archaeal methanogen-produced methane, having values of −50 to −110‰ (33), is a logical candidate for the source of such carbon, a supposition used to explain the occurrence both of the comparably low $\delta^{13}C$ values of carbonaceous matter in pre-2,500 Ma sediments (34, 35) and of modern microbial communities in which, as we infer for the Apex assemblage, anaerobic methane producers and consumers intimately coexist (e.g., refs. 33 and 36).

Incorporation of low $\delta^{13}C$ methane into potentially fossilizable biomass is carried out by γ-proteobacterial methanotrophs, members of the largest class of the Gram-negative proteobacteria (37) among which they are unique in using methane as their sole carbon and energy source (38). However, virtually all such methanotrophs are small single-celled rods, coccoids, or ellipsoids (38, 39) that differ distinctly in cellular morphology from much larger-diameter filamentous specimens of *A. disciformis* and *P. amoenum*. The single exception to this generalization known to us is *Crenothrix polyspora* Cohn 1870, a filamentous bacterium now studied for 150 y (27, 40–42) but only recently shown to be a γ-proteobacterial methanotroph (43, 44), a modern taxon characterized as unbranched filaments composed of cylindrical to disk-shaped cells ∼1 to ∼6 μm broad (27) and thus similar to the 1.8- to 5-μm-diameter quadrate to disk-shaped cell-containing filaments of *A. disciformis* and *P. amoenum* (2).

Regardless of whether *C. polyspora* represents a modern analog of Paleoarchean *A. disciformis* and/or *P. amoenum*—there being insufficient data at present to establish such relationships—the low $\delta^{13}C$ SIMS-documented compositions of these ∼3,465 Ma fossil taxa are most plausibly interpreted as evidencing methanotrophy. This, in turn, requires the presence of biogenic methane produced by Archaeal methanogens, inferred from the SIMS data to have perhaps

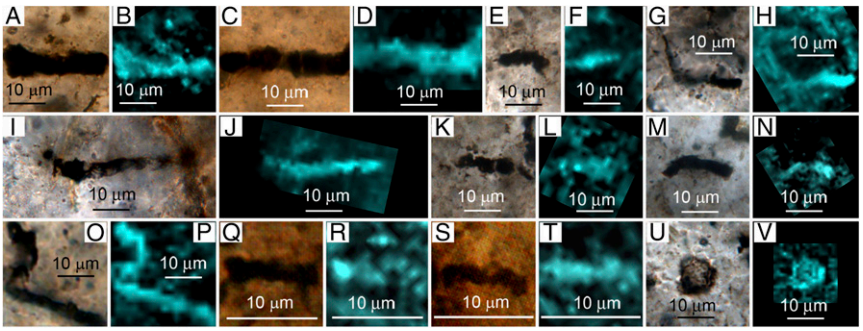

Fig. 2. (*A*, *C*, *E*, *G*, *I*, *K*, *M*, *O*, *Q*, *S*, and *U*) Eleven specimens of five taxa of filamentous microfossils analyzed by SIMS in petrographic thin section 4 of 6/15/82-1H of the ∼3,465 Ma Apex chert shown in transmitted light photomicrographs and (*B*, *D*, *F*, *H*, *J*, *L*, *N*, *P*, *R*, *T*, and *V*) 2D Raman images that document the distribution of kerogen (blue, acquired in a spectral window centered on the kerogen "G" band at ∼1,605 cm^{-1}). (*A–D*) *A. disciformis* Schopf 1993 (*A* and *B*, specimen #F; *C* and *D*, specimen #G). (*E–H*) *P. delicatulum* Schopf 1992 (*E* and *F*, clast specimen #4; *G* and *H*, clast specimen #5). (*I* and *J*) *P. amoenum* Schopf 1992 (specimen #H). (*K–N*) *P. delicatulum* Schopf 1992 (*K* and *L*, clast specimen #6; *M* and *N*, clast specimen #11). (*O–T*) *P. minutum* Schopf 1993 (*O* and *P*, clast specimen #9; *Q* and *R*, small clast specimen #2; *S* and *T*, small clast specimen #3). (*U* and *V*) Unnamed unicell (clast specimen #12).

been generated by taxa such as *P. delicatulum*. Although the SIMS data do not exclude the possible affinity of two of the Apex taxa (an unnamed unicell and *P. minutum*) to phototrophic cyanobacteria and/or photosynthetic bacteria, those of three of the taxa are more plausibly interpreted as evidencing an early-evolved methanogen–methanotroph biocoenose, physiological characteristics compatible with the near-basal position of methane-generating Archaea in rRNA phylogenies (32) and, given the obligate anaerobic metabolism of methanogenic Archaea and the oxygen-deficient setting inhabited by extant methanogen–methanotroph communities (33, 36), consonant also with an anoxic early environment (45, 46).

Conclusions

From the data summarized above (and presented in *Supporting Information*), we interpret these SIMS-based carbon isotope analyses of 11 specimens of five taxa of the ∼3,465 Ma Apex chert of northwestern Western Australia to indicate that (*i*) their taxon-correlated SIMS $\delta^{13}C$ values reinforce both their biogenicity and the widely held assumptions that the organismal and cellular morphology of ancient microbes can be used to establish biologically meaningful taxonomic categories and provide insight into the physiology and biological affinities of the specimens analyzed; (*ii*) two of the taxa exhibit $\delta^{13}C$ compositions not inconsistent with phototrophic metabolism; (*iii*) SIMS data for the other three Apex taxa studied are more compatible with affinities to Archaeal methanogens and γ-proteobacterial methanotrophs, physiological characteristics consonant with the near-basal position of the Archaea in rRNA phylogenies; and (*iv*) the preservation in this ∼3,465 Ma deposit of such Archaea and γ-proteobacteria suggests that methane cycling methanogen–methanotroph communities were a significant component of the Paleoarchean biosphere.

Materials and Methods

Optical Microscopy. Optical images of the thin section-embedded specimens studied here were acquired at the University of California, Los Angeles (UCLA) using fluorescence-free microscopy immersion oil and a Leitz Orthoplan 2 microscope equipped with a Nikon DS Microscope Digital Camera.

Raman Spectroscopy. Molecular structural compositional analyses of the fossils were carried out at UCLA using a T64000 triple-stage confocal laser Raman system that permits acquisition both of point spectra and of Raman images that display the 2D spatial distribution of the molecular structural components of the specimens and their associated minerals, images that can be stacked to provide a 3D image of the specimens analyzed. A Coherent Innova argon ion laser provided excitation at 457.9 nm, permitting data to be obtained over a range from ∼300 cm^{-1} to ∼3,000 cm^{-1} using a single spectral window centered at 1,800 cm^{-1}. The laser power used was ∼6 mW to 8 mW over a ∼1-μm spot, a configuration well below the threshold resulting in radiation damage to kerogenous fossils, and the thin sections were covered by a veneer of fluorescence-free microscopy immersion oil, the presence of which has no discernable effect on the Raman spectra acquired. Varying pixel intensities in the acquired 2D Raman images correspond to the relative concentrations of the material analyzed.

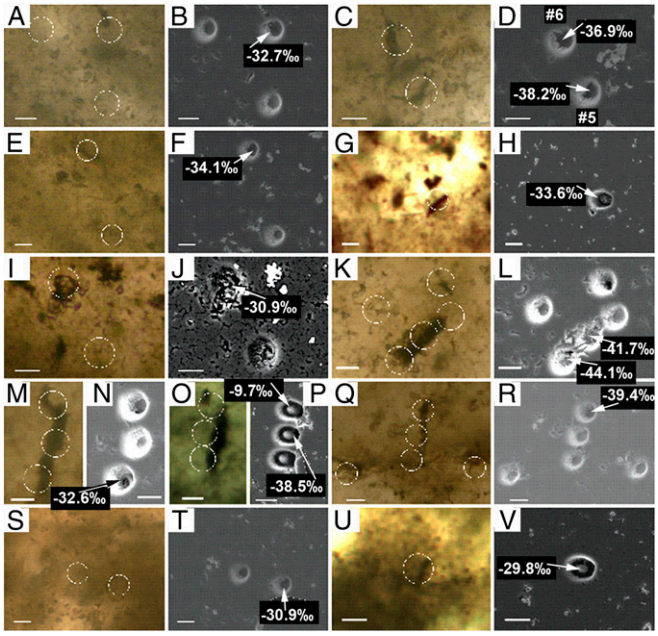

Fig. 3. Paired images of pre-SIMS transmitted light photomicrographs (color) and post-SIMS SEM images (black and white) of 11 specimens of five taxa of microfossils analyzed for $\delta^{13}C$ in petrographic thin section 4 of 6/15/82-1H of the ∼3,465 Ma Apex chert. (*A* and *B*) Clast specimen #4; (*C* and *D*) clast specimens #5 and #6; (*E* and *F*) clast specimen #9; (*G* and *H*) clast specimen #11; (*I* and *J*) clast specimen #12; (*K* and *L*) specimen #F; (*M* and *N*) specimen #G (session-1); (*O* and *P*) specimen #G (session-2); (*Q* and *R*) specimen #H; (*S* and *T*) small clast specimen #2; and (*U* and *V*) small clast specimen #3. White circles in the photomicrographs indicate the locations of the SIMS-produced analytical pits. In the SEM images, *J* is a back-scattered electron image; all others are secondary electron images. These SEM images were acquired in sections veneered with a thin (<∼5-nm-thick) gold coat after removal of a thicker Au coat used during SIMS analyses and show the locations of analyzed spots having high (≥3 Mcps/nA) and marginally accepted (3 Mcps/nA to 1.5 Mcps/nA) ^{12}C yields. Not shown are carbon-poor analytical pits and SIMS-obtained $\delta^{13}C$ measurements considered not to be reliable. See *Supporting Information* for additional analytical data. (Scale bars, 10 μm.)

Table 1. SIMS-determined carbon isotope values of the five taxa of Apex microfossils discussed here

Taxon (specimen)	Figures	Number of measurements	δ^{13}C‰ VPDB*
Unnamed unicell			
(Clast #12)	Figs. 1*N*, 2 *U* and V, and 3 *I* and *J*	1	−30.9
Avg.		(*n* = 1)	−30.9
P. minutum			
(Clast #9)	Figs. 1*K*, 2 *O* and *P*, and 3 *E* and *F*	1	−34.1†
(Small clast #2)	Figs. 1*F*, 2 *Q* and *R*, and 3 *S* and *T*	1	−30.9
(Small clast #3)	Figs. 1*G*, 2 *S* and *T*, and 3 *U* and *V*	1	−29.8
Avg.		(*n* = 3)	−31.6
P. delicatulum			
(Clast #4)	Figs. 1*L*, 2 *E* and *F*, and 3 *A* and *B*	1	−32.7
(Clast #5)	Figs. 1*M*, 2 *G* and *H*, and 3 *C* and *D*	1	−38.2
(Clast #6)	Figs. 1*J*, 2 *K* and *L*, and 3 *C* and *D*	1	−36.9
(Clast #11)	Figs. 1*I*, 2 *M* and *N*, and 3 *G* and *H*	1	−33.6
Avg.		(*n* = 4)	−35.4
A. disciformis			
(Specimen #F)	Figs. 1*C*, 2 *A* and *B*, and 3 *K* and *L*	1	−41.7
(Specimen #F)	Figs. 1*C*, 2 *A* and *B*, and 3 *K* and *L*	1	−44.1‡
(Specimen #G, Session-1)	Figs. 1*B*, 2 *C* and *D*, and 3 *M* and *N*	1	−32.6†
(Specimen #G, Session-2)	Figs. 1*B*, 2 *C* and *D*, and 3 *M* and *N*	1	−38.5§
Avg.		(*n* = 4)	−39.2
P. amoenum			
(Specimen #H)	Figs. 1*D*, 2 *I* and *J*, and 3 *Q* and *R*	1	−39.4
Avg.		(*n* = 4)	−39.4

For detailed summaries of the data, see *Supporting Information*.
*Calibrated vs. VPDB, the "Vienna PDB" standard.
†Marginal ^{12}C-yield spots (see *SIMS*).
‡Repeat analysis.
§Excluding high-δ^{13}C outlier (−9.7‰).

SIMS. At the University of Wisconsin-Madison WiscSIMS Laboratory, analyses of the carbon isotope compositions of the optically and Raman-identified micrometer-sized permineralized fossils in petrographic thin section 4 of 6/15/82-1H were carried out using a SIMS CAMECA IMS 1280. Fossil-containing areas were excised by use of a water-cooled diamond saw, cleaned in ethanol, mounted in epoxy together with two grains of the Bolton scapolite standard (Bolt, Me_{69}; ref. 47), and ground and polished using a water-lubricated diamond paste to expose the target fossils at their surface. Calibration of δ^{13}C was performed using a separate 25-mm-diameter epoxy mount containing the Bolt standard and carbon isotope standard PPRG215 (48, 49). Two types of PPRG215 mounts were used: grain and chip mounts (Figs. S1 and S2). The Bolt standard was calibrated based on PPRG215 and analyzed as a running standard. All mounts were cleaned with ethanol and gold-coated before analyses.

SIMS data were collected in two analytical sessions (Session-1, 5/9/2016 to 5/12/2016; and Session-2, 5/1/2017 to 5/2/2017). Following analysis of each specimen, SIMS pits were imaged by scanning electron microscopy (SEM), and the epoxy mounts were reground and repolished to expose new target fossils at their surface (Fig. S2). After subsequent repolishing and before SIMS analyses, the newly exposed specimens were imaged by optical microscope and SEM.

Analyses of carbon isotope ratios were acquired using a $^{133}Cs^+$ primary ion beam typically having a ∼12-μm-diameter spot size, an intensity of 2.7 nA to 2.9 nA, and a secondary ion accelerating voltage of 10 kV. Details of the analytical conditions used are described by Morag et al. (48). Measurements of the carbon standard mount (Bolt and PPRG215) were performed using the same analytical conditions. To assure the reliability of the results obtained, during the course of the two analytical sessions, the carbon isotope standard was analyzed 190 times (130 spots in Session-1, 60 spots in Session-2; (Figs. S3–S5).

For use of this 12-μm-diameter spot size, external precision was 1.3 to 2.6‰ (2 SD, including the calculated uncertainties of the running and calibration standards, and internal errors). Some of the specimens analyzed contained low concentrations of carbon that yielded low secondary ion count rates having poor analytical precision (Figs. S6 and S7 and Dataset S1). Because the concentration of carbon in the microfossils and that in the chert matrix measured at a distance from the fossils (Fig. 3) was variable, two cutoffs were applied to the acquired data based on the secondary ion ^{12}C count rate: relatively C-rich values, >8.6 Mcps (>3 Mcps/nA), were accepted, whereas values between 8.6 Mcps and 4.3 Mcps (3 Mcps/nA to 1.5 Mcps/nA) were regarded as marginally acceptable. Values less than 4.3 Mcps were regarded as unreliable. Cutoff values were determined by the average count rate of 130 randomly selected spots on carbon standard PPRG215 in two different mounts during analytical Session-1.

Repository of SIMS-Analyzed Specimens. The specimens analyzed here have been archived by J.W.V. in the collections of the Geology Museum of the Department of Geoscience, University of Wisconsin-Madison.

ACKNOWLEDGMENTS. This work is based on the prescience of John M. Hayes, who 35 years ago was first to postulate that the low δ^{13}C values of some Archean kerogens evidence the metabolic consumption of Archaeal-produced methane by γ-Proteobacterial methanotrophs like those here inferred to have been present in the Apex microbial assemblage (34). We thank Chris House (Pennsylvania State University) for providing a sample of carbon isotope standard PPRG215, obtained from the Schopf-curated Precambrian Paleobiology Research Group collections at UCLA; Brian Hess (University of Wisconsin) for skillful attention to the repeated and delicate grinding and polishing required to expose the Apex microfossils at the section surface for SIMS analysis; and Ken Williford (now on the staff of NASA's Jet Propulsion Laboratory) and Navot Morag (now at University of Jerusalem) for assistance in development of the SIMS δ^{13}C standard and of protocols for analyses of kerogens. This research was supported by the National Aeronautics and Space Administration Grant NNA13AA94A issued through the Science Mission Directorate, by the NASA Astrobiology Institute, and by the Center for the Study of Evolution and the Origin of Life at UCLA. WiscSIMS is supported by National Science Foundation Grant EAR-1355590 and University of Wisconsin-Madison.

1. Schopf JW (1992) Paleobiology of the Archean. *The Proterozoic Biosphere, A Multidisciplinary Study*, eds Schopf JW, Klein C (Cambridge Univ Press, New York), pp 25–39.
2. Schopf JW (1993) Microfossils of the early Archean Apex chert: New evidence of the antiquity of life. *Science* 260:640–646.
3. Moorbath S (2005) Palaeobiology: Dating earliest life. *Nature* 434:155.
4. Brasier MD, et al. (2002) Questioning the evidence for Earth's oldest fossils. *Nature* 416:76–81.
5. Brasier MD, et al. (2005) Critical testing of Earth's oldest putative fossil assemblage from the ∼3.5 Ga Apex chert, Chinaman Creek, Western Australia. *Precambrian Res* 140:55–102.
6. García Ruiz JM, Carnerup A, Christy AG, Welham NJ, Hyde ST (2002) Morphology: An ambiguous indicator of biogenicity. *Astrobiology* 2:353–369.
7. García-Ruiz JM, et al. (2003) Self-assembled silica-carbonate structures and detection of ancient microfossils. *Science* 302:1194–1197.

8. Marshall CP, Emry JR, Marshall AO (2011) Haematite pseudomicrofossils present in the 3.5-billion-year-old Apex chert. *Nat Geosci* 4:240–243.
9. Pinti DL, Mineau R, Clement V (2009) Hydrothermal alteration and microfossil artefacts of the 3,465-million-year-old Apex chert. *Nat Geosci* 2:640–643.
10. Brasier MD, Antcliffe J, Saunders M, Wacey D (2015) Changing the picture of Earth's earliest fossils (3.5–1.9 Ga) with new approaches and new discoveries. *Proc Natl Acad Sci USA* 112:4859–4864.
11. Schopf JW, Kudryavtsev AB, Agresti DG, Wdowiak TJ, Czaja AD (2002) Laser–Raman imagery of Earth's earliest fossils. *Nature* 416:73–76.
12. Schopf JW, Kudryavtsev AB (2012) Biogenicity of Earth's earliest fossils: A resolution of the controversy. *Gondwana Res* 22:761–771.
13. Hickman AH, Lipple SL (1978) *Explanatory Notes, Marble Bar 1:250,000 Geological Map Series 24* (Geol Surv West Aust, Perth, Australia).
14. Hickman AH (1983) *Geology of the Pilbara Block and Its Environs* (Geol Surv West Aust, Perth, WA, Australia).
15. Hickman AH (2012) Review of the Pilbara Craton and Fortescue Basin, Western Australia: Crustal evolution providing environments for early life. *Isl Arc* 21:1–31.
16. Van Kranendonk MJ (2006) Volcanic degassing, hydrothermal circulation and the flourishing of early life on Earth: A review of the evidence from c. 3490–3240 Ma rocks of the Pilbara Supergroup, Pilbara Craton, Western Australia. *Earth Sci Rev* 74: 197–240.
17. Pentecost A (2003) Cyanobacteria associated with hot spring travertines. *Can J Earth Sci* 40:1447–1457.
18. Jannasch HW, Wirsen CO (1981) Morphological survey of microbial mats near deep-sea thermal vents. *Appl Environ Microbiol* 41:528–538.
19. Ueno Y, Yoshioka H, Isozaki Y (2004) Carbon isotopes and petrography in ~3.5 Ga hydrothermal silica dykes in the North Pole area, Western Australia. *Geochim Cosmochim Acta* 68:573–589.
20. Rasmussen B (2000) Filamentous microfossils in a 3,235-million-year-old volcanogenic massive sulphide deposit. *Nature* 405:676–679.
21. Ueno Y, Isozaki Y, Yurimoto H, Maruyama S (2001a) Carbon isotopic signatures of individual Archean microfossils(?) from Western Australia. *Int Geol Rev* 43:196–212.
22. Ueno Y, Maruyama S, Isozaki Y, Yurimoto H (2001b) Early Archaean (ca. 3.5 Ga) microfossils and ^{13}C depleted carbonaceous matter in the North Pole area, Western Australia: Field occurrence and geochemistry. *Geochemistry and the Origin of Life*, eds Nakashima S, Maruyama S, Brack A, Windley BF (Universal Academic, New York), pp 203–236.
23. Kiyokawa S, Ito T, Ikehara M, Kitajima F (2006) Middle Archean volcano-hydrothermal sequence: Bacterial microfossil-bearing 3.2-Ga Dixon Island Formation, coastal Pilbara terrain, Australia. *Geol Soc Am Bull* 118:3–22.
24. Schopf JW (2006) Fossil evidence of Archaean life. *Philos Trans R Soc Lond B Biol Sci* 361:869–885.
25. Strauss H, Moore TB (1992) Abundances and isotopic compositions of carbon and sulfur species in whole rock and kerogen samples. *The Proterozoic Biosphere, A Multidisciplinary Study*, eds Schopf JW, Klein C (Cambridge Univ Press, New York), pp 709–798.
26. Schidlowski M, Hayes JM, Kaplan IR (1983) Isotopic inferences of ancient biochemistries: Carbon, sulfur, hydrogen, and nitrogen. *Earth's Earliest Biosphere: Its Origin and Evolution*, ed Schopf JW (Princeton Univ Press, New York), pp 149–186.
27. Buchannan RE, Gibbons NE (1975) *Bergey's Manual of Determinative Bacteriology* (Williams Wilkins, Baltimore), 8th Ed.
28. Schopf JW, Walter MR (1983) Archean microfossils: New evidence of ancient microbes. *Earth's Earliest Biosphere: Its Origin and Evolution*, ed Schopf JW (Princeton Univ Press, New York), pp 214–239.
29. Hofmann HJ, Schopf JW (1983) Early Proterozoic microfossils. *Earth's Earliest Biosphere: Its Origin and Evolution*, ed Schopf JW (Princeton Univ Press, New York), pp 321–360.
30. Burggraf S, Huber H, Stetter KO (1997) Reclassification of the crenarchael orders and families in accordance with 16S rRNA sequence data. *Int J Syst Bacteriol* 47:657–660.
31. Toshchakov SV, et al. (2015) Complete genome sequence of and proposal of *Thermofilum uzonense* sp. nov. a novel hyperthermophilic crenarchaeon and emended description of the genus *Thermofilum*. *Stand Genomic Sci* 10:122–130.
32. Woese CR, Kandler O, Wheelis ML (1990) Towards a natural system of organisms: Proposal for the domains Archaea, Bacteria, and Eucarya. *Proc Natl Acad Sci USA* 87: 4576–4579.
33. Alperin MJ, Hoehler TM (2009) Anaerobic methane oxidation by Archaea/sulfate-reducing bacteria aggregates: 2. Isotopic constraints. *Am J Sci* 309:958–984.
34. Hayes JM (1983) Geochemical evidence bearing on the origin of aerobiosis: A speculative hypothesis. *Earth's Earliest Biosphere: Its Origin and Evolution*, ed Schopf JW (Princeton Univ Press, New York), pp 291–301.
35. Hayes JM (1993) Factors controlling ^{13}C contents of sedimentary organic compounds: Principles and evidence. *Mar Geol* 113:111–125.
36. Ding H, Valentine DL (2008) Methanotrophic bacteria occupy benthic microbial mats in shallow marine hydrocarbon seeps, Coal Oil Point, California. *J Geophys Res Biogeosci* 113:G01015.
37. Woese CR (1987) Bacterial evolution. *Microbiol Rev* 51:221–271.
38. Hanson RS, Hanson TE (1996) Methanotrophic bacteria. *Microbiol Rev* 60:439–471.
39. Whittenbury R, Phillips KC, Wilkinson JF (1970) Enrichment, isolation and some properties of methane-utilizing bacteria. *J Gen Microbiol* 61:205–218.
40. Cohn F (1870) Uber den Brunnenfaden (*Crenothrix polyspora*) mit Bemerkungen fiber die mikroskopische analyse des Brunnenwassers. *Beitr Biol Pflanz* 1:108–131.
41. Harder E (1919) *Iron-Depositing Bacteria and Their Geologic Relations* (US Geol Surv, Washington, DC), Prof Pap 113.
42. Kolk LA (1938) A comparison of the filamentous iron organisms, *Clonothrix fusca* Roze and *Crenothrix polyspora* Cohn. *Am J Bot* 25:11–17.
43. Stoecker K, et al. (2006) Cohn's *Crenothrix* is a filamentous methane oxidizer with an unusual methane monooxygenase. *Proc Natl Acad Sci USA* 103:2363–2367.
44. Vigliotta G, et al. (2007) *Clonothrix fusca* Roze 1896, a filamentous, sheathed, methanotrophic γ-proteobacterium. *Appl Environ Microbiol* 73:3556–3565.
45. Schopf JW, et al. (2017) An anaerobic ~3400 Ma shallow-water microbial consortium: Presumptive evidence of Earth's Paleoarchean anoxic atmosphere. *Precambrian Res* 299:309–318.
46. Farquhar J, Bao H, Thiemens M (2000) Atmospheric influence of Earth's earliest sulfur cycle. *Science* 289:756–759.
47. Moecher DP, Valley JW, Essene EJ (1994) Extraction and carbon isotope analysis of CO_2 from scapolite in deep crustal granulites and xenoliths. *Geochim Cosmochim Acta* 58:959–967.
48. Morag N, et al. (2016) Microstructure-specific carbon isotopic signatures of organic matter from ~3.5 Ga cherts of the Pilbara Craton support a biologic origin. *Precambrian Res* 275:429–449.
49. Williford KH, et al. (2013) Preservation and detection of microstructural and taxonomic correlations in the carbon isotopic compositions of individual Precambrian microfossils. *Geochim Cosmochim Acta* 104:165–182.